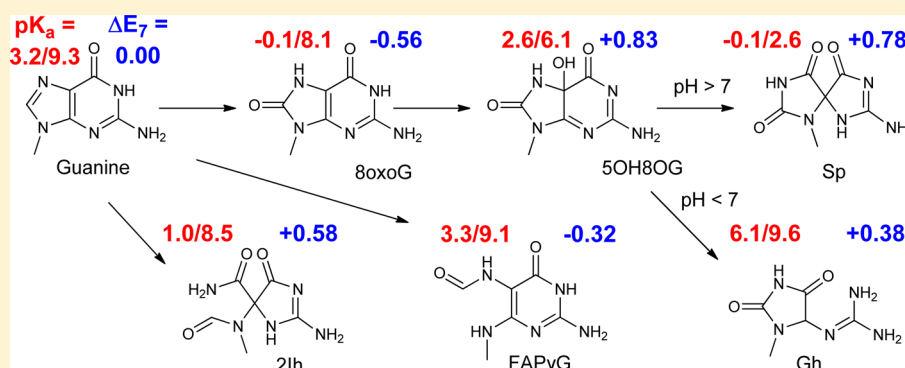# Computational Prediction of One-Electron Reduction Potentials and Acid Dissociation Constants for Guanine Oxidation Intermediates and Products

Brian T. Psciuk and H. Bernhard Schlegel*

Department of Chemistry, Wayne State University, Detroit, Michigan 48202, United States

S *Supporting Information*

ABSTRACT: Reduction potentials and pK_a values were calculated for intermediates and products along three major pathways for guanine oxidation using the B3LYP and CBS-QB3 levels of theory with the SMD implicit solvation model. N-methylated nucleobases were used as models for nucleoside species. Ensemble averaged reduction potentials at pH 7 (E_7) were obtained by combining calculated standard reduction potentials with calculated pK_a values in addition to accounting for tautomerization energies. Calculated pK_a values are reasonable based on experimental estimates and chemical intuition. Pathway A leads to guanidinohydantoin (Gh) and spiroiminodihydantoin (Sp). The first step is the oxidation of 8-oxoguanine which proceeds by the loss of an electron followed by the loss of two protons and loss of another electron, yielding 8-oxopurine. The calculated E_7 values for the remaining intermediates and products are at least 0.3 V higher than that of guanine, indicating that further oxidation of these species is unlikely. Pathway B leads to two formamidopyrimidine isomers (FAPyG and 2,5FAPyG). Species along this pathway have calculated reduction potentials that are much lower than the oxidation potential for guanine and would likely be very short-lived in an oxidatively stressed environment. Pathway C leads to reduced spiroiminodihydantoin and 5-carboxamido-5-formamido-2-iminohydantoin (2Ih). Similar to pathway A, the calculated reduction potentials for species along this pathway are at least 0.4 V higher than that of guanine.

INTRODUCTION

Ionizing radiation and reactive oxygen species are nearly constant sources of oxidative stress to the DNA of living organisms. Oxidative damage to DNA has been implicated in the process of aging, neurological diseases, carcinogenesis, and cellular death.[1−9] Among the canonical nucleobases, guanine is well-known to be the most susceptible to oxidative damage.[10] Extensive research has been carried out over the last few decades to map the reaction pathways following guanine oxidation and to identify the major intermediates and products both experimentally[4,7,11−17] and theoretically.[18−22] The key intermediate and product species examined in this study are based on these experimental and theoretical findings. Figure 1 shows three significant reaction pathways that are available after the initial oxidation of guanine.

Determining the reduction potentials for nucleobase species has been a specific area of research interest to investigators studying oxidative damage to DNA. While there have been numerous experimental studies attempting to accurately measure

a set of absolute reduction potentials for the canonical nucleic acid residues,[10,23−29] the studies by Seidel et al.[25] and Steenken et al.[26,27] are the most widely cited. Standard potentials ($E°$) for the canonical nucleosides were measured in acetonitrile solution by Seidel et al. using cyclic voltammetry. When the potentials in acetonitrile were measured, the possibilities for protonation/deprotonation events were eliminated and the redox pair was strictly between the reduced neutral and the oxidized radical cation. Measurements by Steenken et al. were made in aqueous solution at a specific buffered pH to obtain reduction potentials at a constant pH of 7 (E_7). Redox potentials were obtained by chemical oxidation and kinetic rate measurements of reference compounds reacting with the adenosine, guanosine, and 8-oxoguanosine nucleosides. Environmental factors can further
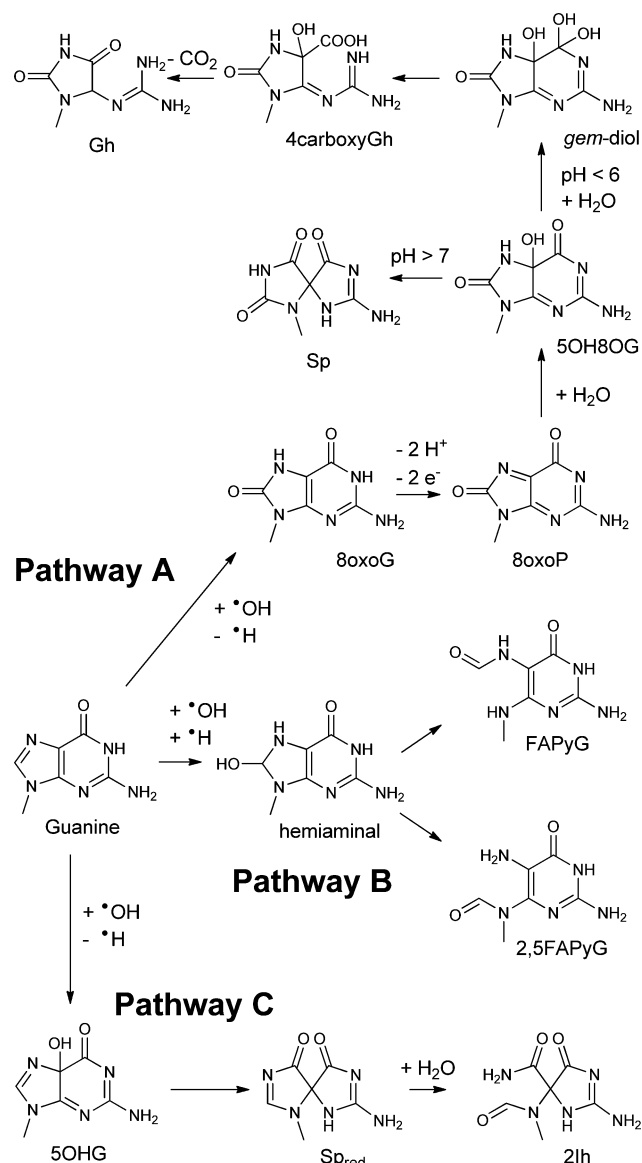
Figure 1. Key intermediates and products along three significant reaction pathways following guanine oxidation. Pathway A starts with the 9-methyl-8-oxoguanine (8oxoG) intermediate structure and leads to the spiroiminodihydantoin (Sp) and guanidinohydantoin (Gh) products. Pathway B goes through the hemiaminal intermediate and produces the formamidopyrimidine (FAPyG) products. Pathway C starts at 5-hydroxy-9-methylguanine (5OHG) and goes through the deoxospiroiminodihydantoin (Sp$_{red}$) intermediate and ends at the 5-carboxamido-5-formamido-2-iminohydantoin (2Ih) product.

complicate the interpretation of redox potentials in connection with oxidative damage to DNA. The redox potentials of guanine, guanosine, and guanosine monophosphate differ by 0.15 V.[30] Phosphate groups can stabilize neighboring radicals by as much as 10 kcal/mol.[31] Base stacking and pairing can change redox potentials by up to 0.3 V.[32,33]

In a previous publication, we developed a computational scheme[34] that reliably reproduced the relative trends in the $E°$ values measured by Seidel et al. and the E_7 values measured by Steenken et al. $E°$ values were obtained from calculated solution phase Gibbs free energies for the redox reactions. E_7 values were computed using the Nernst half-cell equation, which takes into account the physiologically relevant acid dissociation

constants (K_a) for each species in addition to the $E°$ values. Because measured pK_a values were unavailable for many of the one-electron oxidized nucleic acid species, we calculated all the pK_a values needed for the reduced and oxidized species. Using the SMD implicit solvation model with solvent cavity scaling, we achieved good agreement between calculated and measured pK_a values and used the same solvent scaling parameters to reproduce the experimental trends for the $E°$ and E_7 values of nucleosides. For the present study, we employ the same methodology to predict unknown pK_a and E_7 values for key intermediate and product species in the reaction pathways following guanine oxidation. These intermediate and product species may be transient and difficult to isolate experimentally. The thermodynamic properties of many of these species are currently unknown. Accurate prediction of these unknown values could help provide a better understanding of the reaction pathways and mechanisms of oxidative damage.

■ METHODS

A reduction potential under standard conditions is directly proportional to Gibbs free energy of the reaction under the same standard conditions. For a one-electron reduction of the radical cation

$$B^{+\bullet}_{(sol)} + e^- \xrightarrow{\Delta G^*_{red(sol)}} B_{(sol)} \tag{1}$$
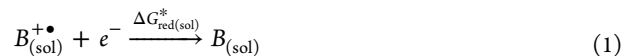
the standard reduction potential is

$$E°_{red(sol)} = \frac{-\Delta G^*_{red(sol)}}{F} \tag{2}$$

where F is Faraday's constant (23.06 kcal/mol). The Gibbs energy of reducing the radical cation species in solution

$$\Delta G^*_{red(sol)} = G^*_{(sol)}(B) - G^*_{(sol)}(B^{+\bullet}) - G°_{(g)}(e^-) \tag{3}$$

is calculated with the aid of a thermodynamic cycle shown in Scheme 1. The standard state Gibbs energy in solution

$$G^*_{(sol)} = (G°_{(g)} + \Delta G^{1atm \to 1M}) + G^*_{solv} \tag{4}$$

Scheme 1. Thermodynamic Cycle Used in the Calculation of Reduction Potentials
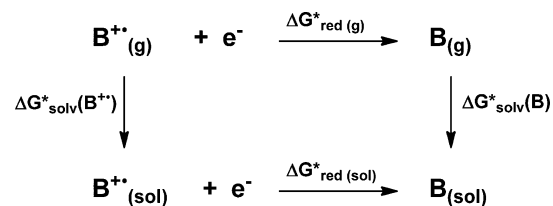
is the sum of the standard state Gibbs energy in the gas phase $G°_{(g)}$ and the standard state Gibbs energy of solvation G^*_{solv} with an additional term, $\Delta G^{1 atm \to 1M} = 1.89$ kcal/mol, for converting from the standard state concentration of 1 atm in the gas phase to the standard state concentration of 1 mol/L in the solution phase. Using the notation introduced by Ben-Naim and Marcus,[35] the standard state at 1 atm is denoted by a degree symbol (°) and the standard state at 1 mol/L is denoted by an asterisk (*). As outlined in Scheme 1, the Gibbs energy for the reduction reaction in solution is

$$\Delta G^*_{red(sol)} = (G°_{(g)}(B) + \Delta G^{1atm \to 1M} + \Delta G^*_{solv}(B))$$
$$- (G°_{(g)}(B^{+\bullet}) + \Delta G^{1atm \to 1M} + \Delta G^*_{solv}(B^{+\bullet})) - G°_{(g)}(e^-) \tag{5}$$

Experimental potentials are measured or referenced against a standard electrode and reported as relative half-cell potentials. To convert calculated absolute reduction potentials to standard reduction potentials, the estimated absolute potential of the standard hydrogen electrode (SHE = 4.281 V)[36−39] is subtracted from the computed potential calculated using eq 2. Our previous investigation found that there were still systematic differences in the calculated potentials relative to the SHE compared to the measured potentials. In this study, all calculated potentials will be reported relative to the calculated guanine potential.

The calculated gas phase Gibbs energy is

$$G_{(g)}^{\circ} = E_{el} + ZPE + \Delta G_{0 \to 298K}^{\circ} \tag{6}$$

where E_{el} is the computed electronic energy including nuclear repulsion, ZPE the zero point vibrational energy, and $\Delta G_{0 \to 298K}^{\circ}$ the calculated increase in the Gibbs energy from 0 to 298 K based on ideal gas approximations. Gas phase structures are optimized using the B3LYP hybrid density functional[40−44] with the 6-31+G(d,p) basis set.[45−50] Vibrational frequency calculations at this geometry are used to compute the ZPE and $\Delta G_{0 \to 298K}^{\circ}$ energies. E_{el} is obtained from a single-point calculation with the larger aug-cc-pVTZ basis set[51] using the gas phase optimized geometry. The computational procedure for obtaining the gas phase Gibbs energy is

$$G_{(g)}^{\circ} = E_{el}^{B3LYP/aug-cc-pVTZ//B3LYP/6-31+G(d,p)} + ZPE^{B3LYP/6-31+G(d,p)}$$
$$+ \Delta G_{0 \to 298K}^{\circ B3LYP/6-31+G(d,p)} \tag{7}$$

A more accurate approach for computing gas phase Gibbs energies is also employed using the CBS-QB3 compound model chemistry,[52,53] which has been shown to produce nearly chemically accurate gas phase thermodynamic energies (mean absolute error of 1.1 kcal/mol).

The Gibbs energy of solvation for a given molecule is the difference between the solution phase Gibbs energy of a solution phase optimized molecule (R') and the gas phase Gibbs energy of a gas phase optimized molecule (R).

$$\Delta G_{solv}^{*} = G_{(sol)}^{*}(R') - G_{(g)}^{*}(R) \tag{8}$$

Solution phase Gibbs energies are computed at the B3LYP/6-31+G(d,p) level of theory using the SMD implicit solvation model.[54] The SMD implicit solvation model[54] includes electrostatic, cavitation, and dispersion energies. SMD uses the integral equation formalism of the polarizable continuum model (IEF-PCM)[55−58] with a parametrized set of atomic radii to calculate the bulk electrostatic energy contribution. Solute−solvent short-range interactions are calculated using a modified solvent-accessible area with parameters for atomic and molecular surface tensions and hydrogen bond acidity and basicity. An average tesserae area of 0.2 Å^2 is used for the tessellated solute−solvent boundary.

Combining the gas phase Gibbs energies with the SMD solvation Gibbs energies calculated yields the B3LYP solution phase Gibbs energies

$$G_{(sol)}^{*} = E_{el}^{B3LYP/aug-cc-pVTZ//B3LYP/6-31+G(d,p)}$$
$$+ ZPE^{B3LYP/6-31+G(d,p)} + \Delta G_{0 \to 298K}^{B3LYP/6-31+G(d,p)} + \Delta G^{1atm \to 1M}$$
$$+ \Delta G_{solv}^{*SMD/B3LYP/6-31+G(d,p)} \tag{9}$$

and the CBS-QB3 solution phase Gibbs energies

$$G_{(sol)}^{*} = G_{(g)}^{CBS-QB3} + \Delta G^{1atm \to 1M} + \Delta G_{solv}^{*SMD/B3LYP/6-31+G(d,p)} \tag{10}$$

All calculations in this study were performed with the development version of the Gaussian series of programs.[59]

Our previous study[34] found that reliable relative reduction potentials and pK_a values could be computed using N-methylated nucleobases (N9 for pyrimidines and N1 for purines shown in Scheme 2) as models for nucleosides and

Scheme 2. Atomic Numbering for Purine and Pyrimidine Nucleobases
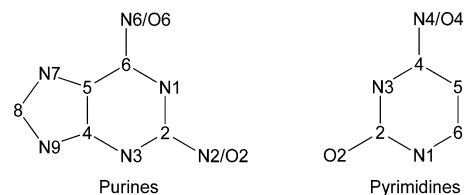
nucleotides. While the effect of the sugar moiety on the absolute reduction potential for the nucleic acid species is debatable, the influence on the relative reduction potentials should be small because the valence molecular orbitals involved in the redox process are localized on the base. Because the hydroxyl groups of the sugar are deprotonated only under very basic conditions (pH > 12), N-methylated nucleobases should also be good models for the protic equilibria of nucleosides near physiological pH.

For biological environments, the reduction potentials under standard conditions at pH 0, E°, are not as relevant as the reduction potentials at pH 7, E_7. The Nernst half-cell equation

$$E_{1/2} = E^{\circ} - \frac{RT}{F} \ln\left(\frac{[Red]}{[Ox]}\right) \tag{11}$$

can be used convert standard potentials to other conditions. For the reduction potential at pH 7 in aqueous solution, the equilibrium concentrations of the physiologically relevant protonation states must be obtained using the acid dissociation constants (K_a). Assuming dilute concentrations of the solute and low ionic strength, an example equation of a pH-dependent potential is[60,61]

$$E_{pH} = E^{\circ}(X^{\bullet}, H^{+}/XH) + \frac{RT}{F} \ln\left(\frac{K_{a1o}}{K_{a1r}}\right)$$
$$+ \frac{RT}{F} \ln\left(\frac{K_{a1r}K_{a2r} + K_{a1r}10^{-pH} + 10^{-2pH}}{K_{a1o} + 10^{-pH}}\right) \tag{12}$$

The standard redox pair in eq 12 involves a one-electron redox event and a change in protonation state where XH is the reduced neutral form of the nucleobase species and $X^{\bullet}$ is the neutral oxidized radical that has one less proton than the reduced neutral species. In a physiological environment where the pH of the aqueous solution is near 7, the neutral forms of the reduced and oxidized nucleobases tend to be dominant; therefore, the redox reaction for E° is immediately followed by a proton transfer. The acid dissociation constants for the oxidized and reduced species are identified by subscripts "o" and "r", respectively. The K_a subscript number indicates the ordering of the deprotonation events from acidic to basic; for example, the first physiologically relevant deprotonation event
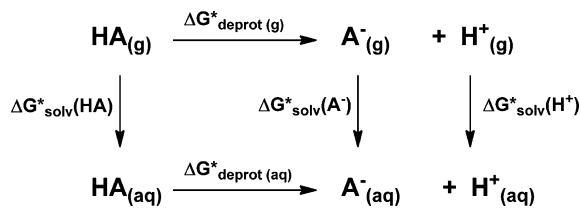
for the reduced species of a given nucleobase is signified by K_{a1r}. Further details about the derivation of eq 12 and additional discussions regarding pH-dependent potentials can be found in the literature.[60,61]

For most of the intermediate and product species along the guanine oxidation pathways, experimental measurements of pK_a values are not available. This is especially true for oxidized species. Because these pK_a values are required for evaluating the E_7 values, we calculated the relevant pK_a values for each of the intermediate and product species. Similar to reduction potentials, the pK_a values are directly proportional to the Gibbs energy for deprotonation

$$pK_a = \frac{\Delta G^*_{deprot(aq)}}{2.303RT} \qquad (13)$$

Scheme 3 describes the thermodynamic cycle used to calculate $\Delta G^*_{deprot\,(aq)}$. In the calculation of the Gibbs energy for aqueous deprotonation of a given species, HA,

**Scheme 3. Thermodynamic Cycle Used in the Calculation of pK_a Values**

$$\Delta G^*_{deprot(aq)} = (G^o_{(g)}(A^-) + \Delta G^{1atm \to 1M} + \Delta G^*_{solv}(A^-))$$
$$+ (G^o_{(g)}(H^+) + \Delta G^{1atm \to 1M} + \Delta G^*_{solv}(H^+))$$
$$- (G^o_{(g)}(HA) + \Delta G^{1atm \to 1M} + \Delta G^*_{solv}(HA)) \qquad (14)$$

the aqueous solvation Gibbs energy of a proton is given by the literature value $\Delta G^*_{solv}(H^+) = 265.9$ kcal/mol.[62]

Nucleobases contain multiple sites for protonation or deprotonation. In an aqueous solvent environment, multiple tautomers of a given nucleobase will be present in equilibrium concentrations for both the reduced and oxidized species (Scheme 4).

Scheme 4. Multiple Tautomers Contribute to the Ensemble Reduction Potential
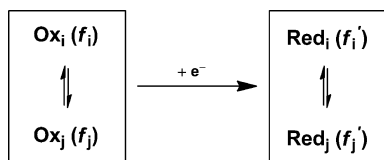
To model experimental measurements in aqueous solution, all of the significantly populated tautomers must be taken into account. Using the Boltzmann populations for each tautomer

$$f_1 = \frac{\exp\left(\frac{-G^*_{1(sol)}}{RT}\right)}{\sum_n \exp\left(\frac{-G^*_{n(sol)}}{RT}\right)} \quad \text{where} \quad \sum f_n = 1 \qquad (15)$$

the ensemble averaged reduction potential is

$$E^o_{red(sol)} = E^o_{red(sol)}{}^{ij} + \frac{RT}{F}\ln(f_i) - \frac{RT}{F}\ln(f_j') \qquad (16)$$
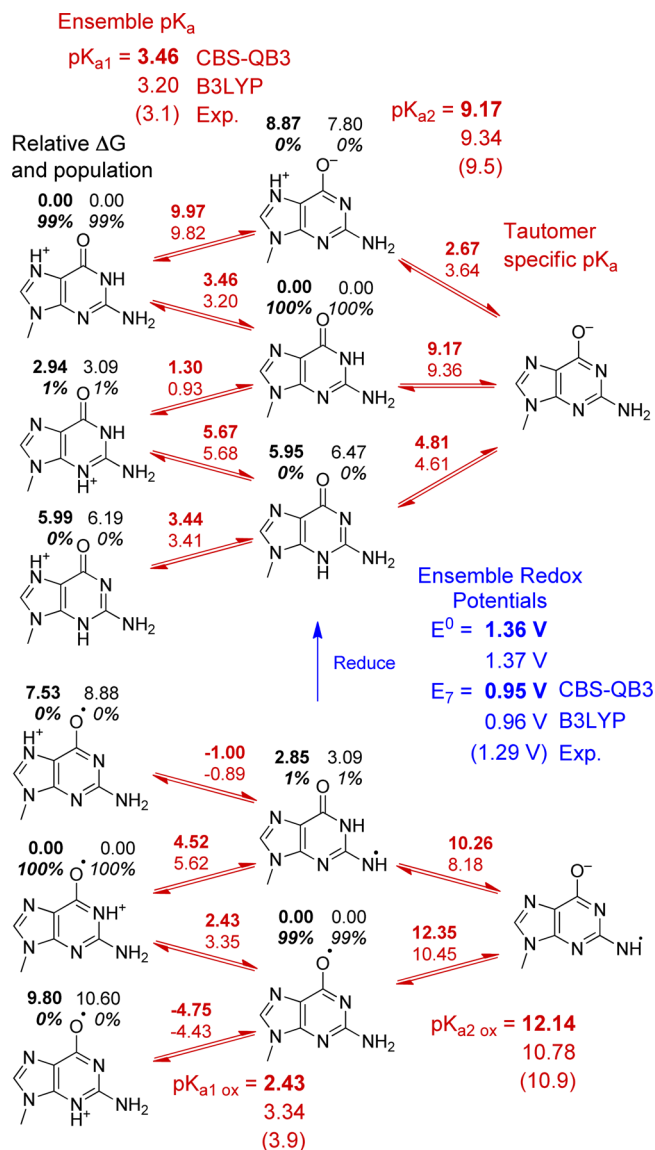
Figure 2. Calculated pK_a values and reduction potentials for 9-methylguanine (G). Where applicable, relative Gibbs free energy differences in kilocalories per mole (black) with the tautomer populations (black italics) are shown near individual tautomers. Tautomer specific pK_a values (red) are shown between individual isomers. Ensemble averaged pK_a values (red) are shown at the top and bottom of the figure. Ensemble oxidation potentials E^o and E_7 (blue) are shown between the reduced and oxidized species on the right. Figures 3−15 report oxidation potentials relative to guanine (E^o_{rel} and $E_{7\,rel}$). Experimentally measured values are shown in parentheses.

where $E^{oij}_{red(sol)}$ is the tautomer specific reduction potential, f_i the population of the i-th tautomer of the oxidized species, and f_j' the j-th tautomer of the reduced species. Similarly, the ensemble pK_a value is

$$pK_a = pK_a{}^{xy} - \log(f_x) + \log(f_y') \qquad (17)$$

where $pK_a{}^{xy}$ is the tautomer specific pK_a and f_x is the population of the species that is protonated relative to the deprotonated species that has a population f_y'.

For the tautomeric sampling, as many as four low-energy tautomers were examined per protonation state for each reduced and oxidized species; though in most cases, only one or two tautomers needed to be considered. Tautomers that included

Table 1. Calculated Reduction Potentials and pK_a values for Reactant, Intermediate, and Product Species Using B3LYP and CBS-QB3 Methodologies

species	methodology	pK_{a1}	pK_{a2}	p$K_{a1\ ox}$	p$K_{a2\ ox}$	$E°_{rel}$	$E_{7\ rel}$
G							
	B3LYP	3.20	9.34	3.34	10.78	0.00 (1.37)[a]	0.00 (0.96)[a]
	CBS-QB3	3.46	9.17	2.43	12.14	0.00 (1.36)[a]	0.00 (0.95)[a]
8oxoG							
	B3LYP	−0.12	8.13	−0.28	5.50	−0.45	−0.56
	CBS-QB3	0.01	7.19	0.05	4.97	−0.41	−0.53
8oxoP							
	B3LYP	−0.04	7.52	−1.92		+1.13	+1.13
	CBS-QB3	1.21	8.25				
5OH8OG							
	B3LYP	2.56	6.05	2.31	1.17	+0.77	+0.83
	CBS-QB3	3.75	6.69	5.23	0.69	+1.08	+1.15
gem-diol							
	B3LYP	7.40	6.69	1.48	5.07	+0.44	+0.48
	CBS-QB3	8.33	7.89	5.53	5.85	+0.70	+0.78
4carboxyGh							
	B3LYP	−2.59	6.07	3.88	9.11	+1.06	+1.11
	CBS-QB3	−0.44	6.66	7.61	7.81	+1.25	+1.23
Gh							
	B3LYP	6.11	9.58	2.29	7.60	+0.38	+0.38
	CBS-QB3	7.77	9.14	0.70	9.89	+0.44	+0.49
Sp							
	B3LYP	−0.06	2.64	−4.26	0.53	+0.53	+0.78
	CBS-QB3	1.32	3.30	−0.74	−0.32	+0.72	+0.93
hemiaminal							
	B3LYP	2.62	9.53	5.45	13.59	−0.84	−0.84
	CBS-QB3	2.49	7.92	6.16	11.02	−0.75	−0.75
FAPyG							
	B3LYP	3.29	9.06	5.41	8.08	−0.32	−0.32
	CBS-QB3	3.66	8.40	6.58	8.08	−0.24	−0.25
2,5FAPyG							
	B3LYP	2.77	7.40	4.11	8.61	−0.54	−0.54
	CBS-QB3	3.10	7.04	4.43	8.58	−0.43	−0.42
5OHG							
	B3LYP	2.77	8.03	4.11		+0.81	+0.81
	CBS-QB3	3.69	9.44	4.81		+1.05	+1.05
Sp$_{red}$							
	B3LYP	0.49	7.40		6.72	+0.45	+0.45
	CBS-QB3	1.40	7.12		6.02	+0.61	+0.62
2Ih							
	B3LYP	0.95	8.49	−2.35	5.85	+0.58	+0.58
	CBS-QB3	2.40	8.18	−4.58	5.55	+0.69	+0.69

[a]Numbers in parentheses are for reduction potentials referenced to SHE.

protonated amino groups (e.g., −NH$_3^+$) and enol forms of keto structures were typically found to be much higher in energy and were not included in the tautomeric sampling. Multiply charged species were not considered because they are unlikely to be relevant.

Our previous study[34] found that standard implicit solvent methods were not sufficiently accurate for redox and pK_a calculations because of specific solvent interactions with charged solutes. To overcome these inaccuracies in solvation modeling, we scaled the solute cavity for charged species to obtain a best fit between our calculated pK_a values and well-established experimentally measured pK_a values for the nucleobases. Cavity scaling parameters for B3LYP were 1.00 for cations and 0.90 for anions; the scaling parameters for CBS-QB3 were 0.975 for cations and 0.925 for anions; cavities for neutral molecules were

not scaled. Because the guanine oxidation pathway intermediate and product species are sufficiently similar to the canonical nucleobases from the previous study, we used the same cavity scaling parameters for all the species in this study.

■ RESULTS AND DISCUSSION

Details of the present calculations of pK_a values and reduction potentials of the intermediates and products along the guanine oxidation pathways are presented in Figures 2−15, and are summarized in Table 1. The calculated pK_a values for guanine (pK_{a1} 3.20, pK_{a2} 9.34 at B3LYP and pK_{a1} 3.46, pK_{a2} 9.17 at CBS-QB3)[34,34,34,32,31,30] are in excellent agreement with other calculated values (pK_{a1} 3.4,[63] 3.15;[64] pK_{a2} 9.6,[63] 9.60[64]) and experimental measurements (pK_{a1} 3.1, pK_{a2} 9.5).[65] Similarly, our calculated pK_a values for oxidized guanine (p$K_{a1\ ox}$ 3.34,

$pK_{a2 ox}$ 10.78) are also in excellent agreement with calculated ($pK_{a1 ox}$ 4.01[66]) and experimental values ($pK_{a1 ox}$ 3.9,[67] $pK_{a2 ox}$ 10.9[67]). The contributing tautomers were also consistent with those found experimentally, where the pK_{a1} is a deprotonation at the N7 position, the pK_{a2} and $pK_{a1 ox}$ are deprotonations from the N1 position, and the $pK_{a2 ox}$ is a deprotonation from the N2 amino group.

Guanine is the most easily oxidized of the canonical nucleobases. The most widely cited value for guanine is 1.29 V,[26] obtained by Steenken from chemical oxidation and kinetic rate measurements on the nucleoside in aqueous solution. By contrast, Faraggi et al.[24] measured 1.06 V for 1-methylguanine by cyclic voltammetry. Our calculations on 9-methyl guanine at the CBS-QB3 and B3LYP levels of theory yield 0.95 and 0.96 V. As discussed in our previous study,[34] better agreement between computed and experimental values can be obtained for reduction potential differences between the nucleobases than for reduction potentials relative to SHE. The computations have difficulty in obtaining accurate estimates of solvation energies for ionic species; the experiments are hampered by problems with solubility and irreversibility; environmental effects routinely shift the redox potentials. When differences are taken, many of these systematic biases cancel. For example, the calculated difference between the reduction potentials of methyl-substituted guanine and 8-oxoguanine (−0.53 V at CBS-QB3 and −0.56 V at B3LYP) is in very good agreement with experiment for guanosine and 8-oxoguanosine (−0.55 V).[26,27] Therefore, discussion of reduction potentials in this study will be based on values relative to the reduction potential of guanine at pH 7, and are denoted as $E_{7 rel}$. Because all reduction potentials and pK_a values were computed using two theoretical methods, the numbers are reported as a range of values in the discussion.

Following the initial oxidation of guanine, three significant reaction pathways are considered in the present study, identified as A, B, and C in Figure 1. Key intermediates and products were chosen based on pathways deduced from experimental investigations[4,7,11,13−17] and computational investigations of the energetics of the guanine oxidation reaction pathways (for leading computational references, see work by Wetmore et al.[19] and by Munk et al.[20−22]).

Pathway A. This pathway starts with 9-methyl-8-oxoguanine (8oxoG), which can be formed by the attack of a reactive oxygen species at the C8 position of guanine (G). As shown in Table 1 and Figure 3, the calculated pK_a values of 8oxoG (pK_{a1} −0.12, pK_{a2} 8.13, $pK_{a1 ox}$ −0.28, and $pK_{a2 ox}$ 5.50)[34] are in good agreement with experimental measurements (pK_{a1} 0.1,[68] pK_{a2} 8.6,[68] and $pK_{a2 ox}$ 6.6[27]) and other calculated results (pK_{a1} −0.4,[63] pK_{a2} 8.0,[63] pK_{a1} 0.22,[69] and pK_{a2} 8.69[69]). Ring nitrogen atoms in cationic 8oxoG are all protonated, and the first deprotonation occurs at the N3 position. The reduced neutral and radical cation species are identical isomers, but deprotonation for pK_{a2} occurs at N1 while deprotonation for $pK_{a1 ox}$ occurs at N7. The $pK_{a2 ox}$ involves the deprotonation of the last protonated ring nitrogen at N1. Our calculated E_7 value for 8oxoG is 0.53−0.56 V lower than that for G,[34] in very good agreement with the experimental difference in reduction potentials (0.55 V).[26,27] Although 8oxoG is a stable intermediate along the path, its low reduction potential relative to G indicates that 8oxoG can easily undergo further oxidation. At pH 7, the oxidation of the canonical nucleobases is accompanied by the loss of a proton. The calculated pK_a values for oxidized 8oxoG show that it will lose not just one proton but also a second proton to form the radical anion at physiological pH. Loss of an
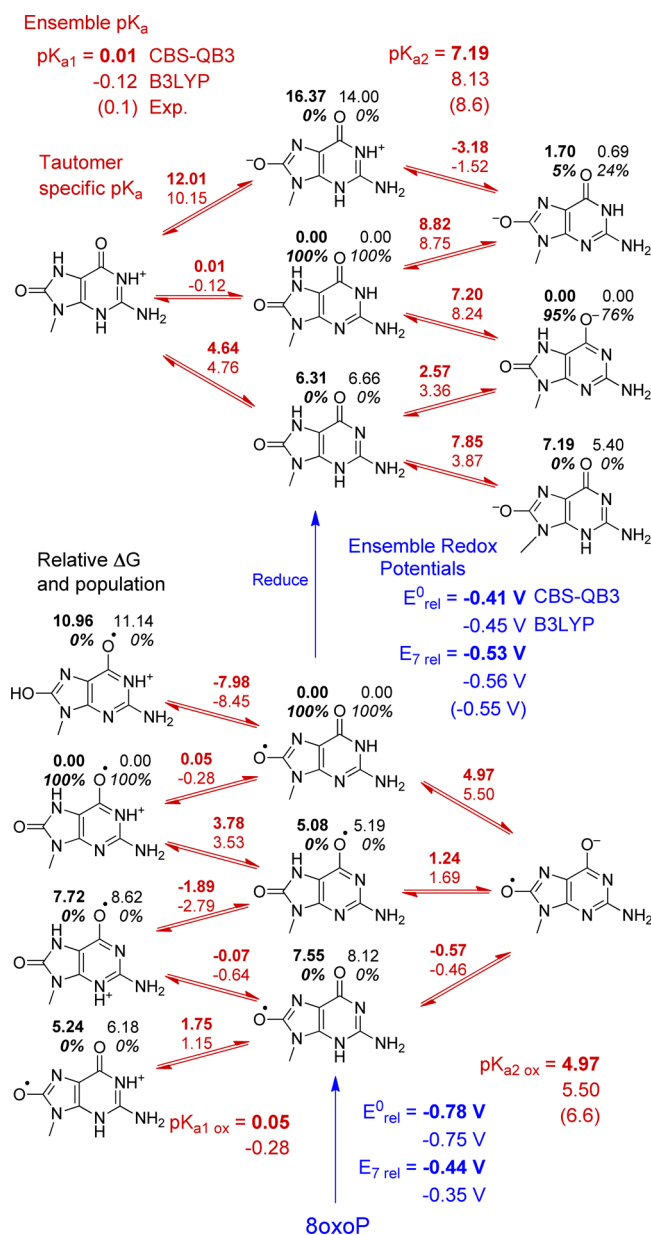

Figure 3. Calculated pK_a values and relative reduction potentials for 9-methyl-8-oxoguanine (8oxoG). See Figure 2 caption for details. Blue values at the bottom of the figure are the relative $E°$ and E_7 values for the oxidized 8oxoG and reduced 8oxoP one-electron redox pair.

additional electron from oxidized 8oxoG yields 2-amino-6,8-dioxo-9-methylpurine (8oxoP). The calculated reduction potential of oxidized 8oxoG is 0.35−0.44 V lower than that of G. This indicates the oxidation of 8oxoG to 8oxoP can occur readily by the removal of an electron, followed by the loss of two protons and then removal of one more electron.

The pK_a values for 8oxoP (Figure 4) are very similar to those of 8oxoG: pK_{a1} is 0.0−1.2, pK_{a2} 7.5−8.2, and $pK_{a1 ox}$ ca. −2. However, the protonation sites of 8oxoP differ from 8oxoG: for pK_{a1}, deprotonation takes place at N1, while for pK_{a2} and $pK_{a1 ox}$ it occurs at the exocyclic N2 amine position. The CBS-QB3 calculations of $pK_{a1 ox}$ and the reduction potentials are unreliable because of severe spin contamination. Because 8oxoP has already been oxidized twice from 8oxoG, the reduction potential is expected to be comparatively high, and further oxidation is unlikely. The calculated E_7 of 8oxoP is 1.1 V higher
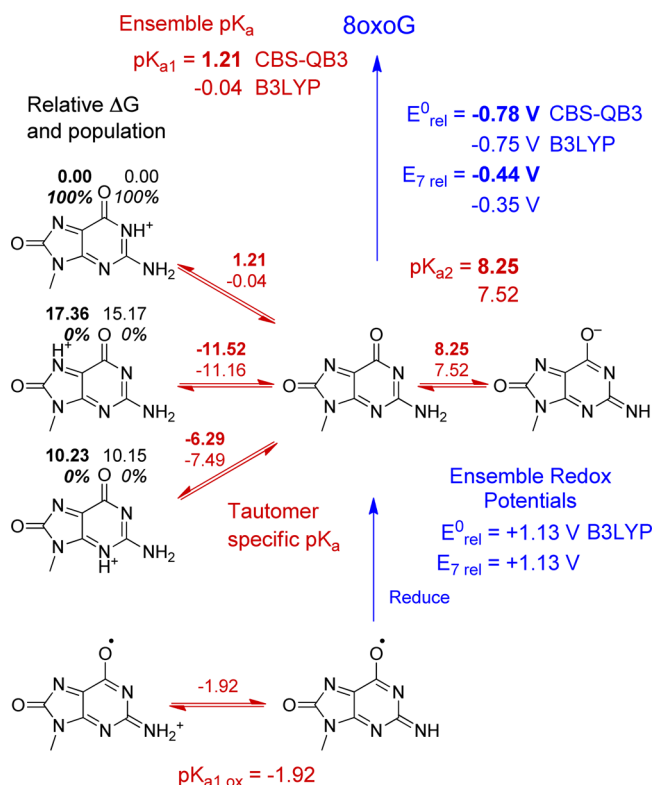
9523

dx.doi.org/10.1021/jp4062412 | J. Phys. Chem. B 2013, 117, 9518−9531

Figure 4. Calculated pK_a values and relative reduction potentials for 2-amino-6,8-dioxo-9-methylpurine (8oxoP). See Figure 2 caption for details. Blue values at the top of the figure are the relative $E°$ and reduction potentials for the oxidized 8oxoG and reduced 8oxoP one-electron redox pair.

Figure 5. Calculated pK_a values and relative reduction potentials for 5-hydroxy-9-methyl-8-oxoguanine (5OH8OG). See Figure 2 caption for details.

than that of guanine and 0.4 V higher than the calculated E_7 of uracil,[34] which has the highest reduction potential of the canonical nucleobases. The next step on the reaction pathway involves the addition of water across the C4—N7 bond of 8oxoP, leading to the 5-hydroxy-9-methyl-8-oxoguanine (5OH8OG) intermediate. This step is calculated to have a reaction Gibbs energy of ca. −5 to +1 kcal/mol.

5OH8OG is a key intermediate step along pathway A for guanine oxidation where a pH-dependent bifurcation of the reaction path takes place. A recent study by Burrows and co-workers[70] investigating the environmental effects on the guanine oxidation pathway inferred a pK_a of ∼5.7 for the 5OH8OG nucleoside based on product yield ratios. This pK_a is the critical factor in determining that the reaction proceeds to guanidinohydantoin (Gh) under acidic conditions (pH < 5.7) and to spiroiminodihydantoin (Sp) under neutral to basic conditions (pH > 5.7). In a theoretical study detailing the energetics of guanine oxidation pathways, Munk et al.[21] found that the lowest energy route for converting 8oxoG to Sp involved an initial deprotonation of neutral 5OH8OG followed by the migration the C6—O6 acyl group from C5 to C4. Figure 5 shows that 5OH8OG protonates at N1 with a pK_{a1} of 2.56−3.75, which is similar to the first protonation of guanine. The computed pK_{a2} of 6.05−6.69 is in good agreement with 5.7 deduced by Burrows, and supports both the experimental and calculated results that the conversion of 5OH8OG to Sp occurs under neutral to basic conditions. Acyl migration converts deprotonated 5OH8OG to deprotonated Sp and is exothermic by ca. 24−25 kcal/mol. Under mildly acidic conditions, 5OH8OG is uncharged. The addition of water to the C6
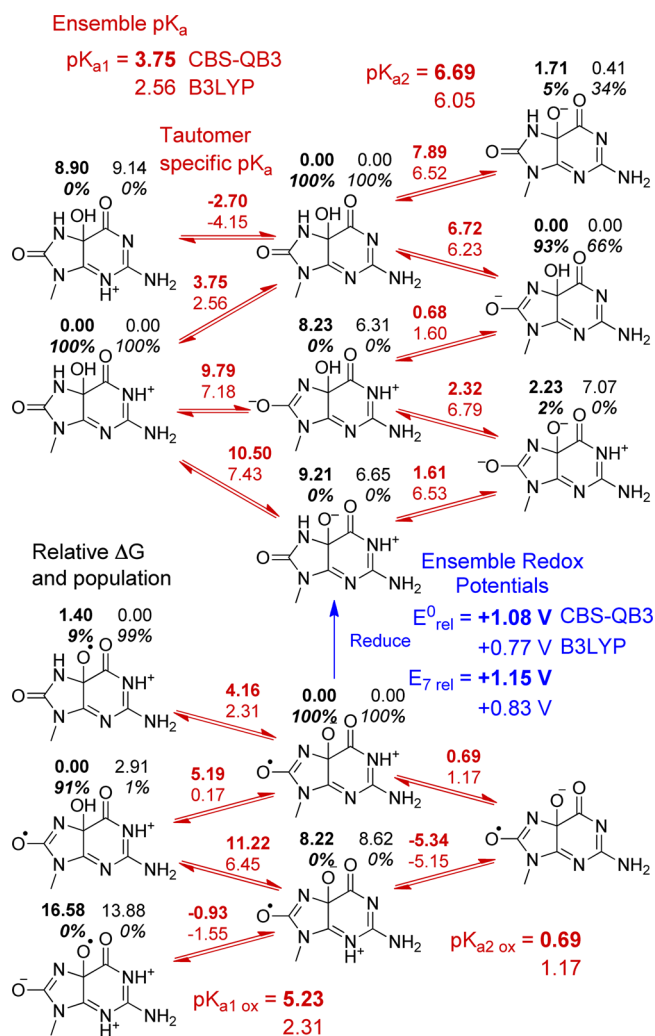
carbonyl generates the *gem*-diol intermediate on the pathway toward Gh. The formation of the *gem*-diol from 5OH8OG is endothermic by ca. 12−22 kcal/mol for the neutral case and ca. 6−15 kcal/mol for the N1 protonated case.

The estimation of E_7 of 5OH8OG requires the pK_a values of the oxidized species. Two tautomers of the radical cation of 5OH8OG are within 3 kcal/mol energetically for each level of theory (however, B3LYP and CBS-QB3 differ in the preferred site of protonation). Only zwitterion structures could be optimized for the neutral radical, and both levels of theory agree that N1 is protonated (optimization of nonzwitterionic structures of the neutral radical in the gas phase resulted in ring-opening at the C5−C6 bond). The B3LYP level of theory predicts a p$K_{a1\ ox}$ of 2.31, which is similar to the p$K_{a1\ ox}$ of guanine. The calculated E_7 value for 5OH8OG is 0.83−1.15 V higher than that of guanine, and thus 5OH8OG is not susceptible to further oxidation.

Addition of water to the C6−O6 carbonyl of 5OH8OG is endothermic by ca. 12−22 kcal/mol and yields the *gem*-diol intermediate (Figure 6). The *gem*-diol intermediate prefers a cationic state as reflected by the unusually high pK_{a1} of 7.40−8.33 involving an N1 deprotonation. The calculated pK_{a2} is 6.69−7.89 and is predicted to be lower than the calculated pK_{a1}. The deprotonation associated with pK_{a2} leads to four tautomers
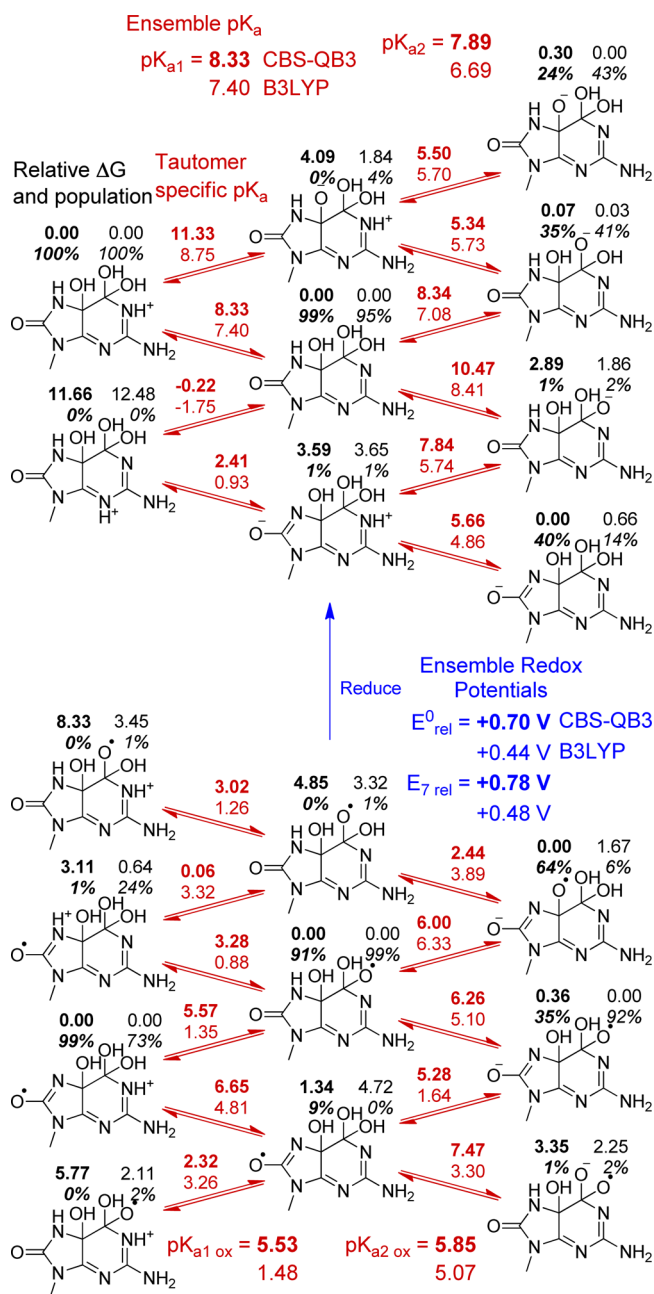
Figure 6. Calculated pK_a values and relative reduction potentials for *gem*-diol. See Figure 2 caption for details.

Figure 7. Calculated pK_a values and relative reduction potentials for 4-carboxy-1-methylguanidinohydantoin (4carboxyGh). See Figure 2 caption for details. Calculations show that if the carboxylic acid of oxidized 4carboxyGh is deprotonated, the molecule will dissociate into carbon dioxide and Gh.

that are very similar in energy. The calculated pK_a values for the oxidized *gem*-diol are 1.48−5.53 for p$K_{a1 ox}$ and 5.07−5.85 for p$K_{a2 ox}$. The *gem*-diol has a calculated E_7 which is 0.48−0.78 V higher than that of guanine, indicating further oxidation is unlikely.

The next step on pathway A toward Gh is a ring-opening and proton transfer, converting the *gem*-diol to the 4-carboxy-9-methylguanidinohydantoin (4carboxyGh) intermediate. This step is 15−23 kcal/mol exothermic for the neutral species. Neutral 4carboxyGh (Figure 7) is a zwitterion with a negatively charged carboxylate and a positively charged guanidine group. Protonation occurs at the carboxyl group with a calculated pK_{a1} of −0.44 to −2.59. Deprotonation occurs at N7 of the neutral species with a pK_{a2} of 6.07−6.66, and the guanidine group is predicted to remain positively charged. Deprotonation of the radical cation at
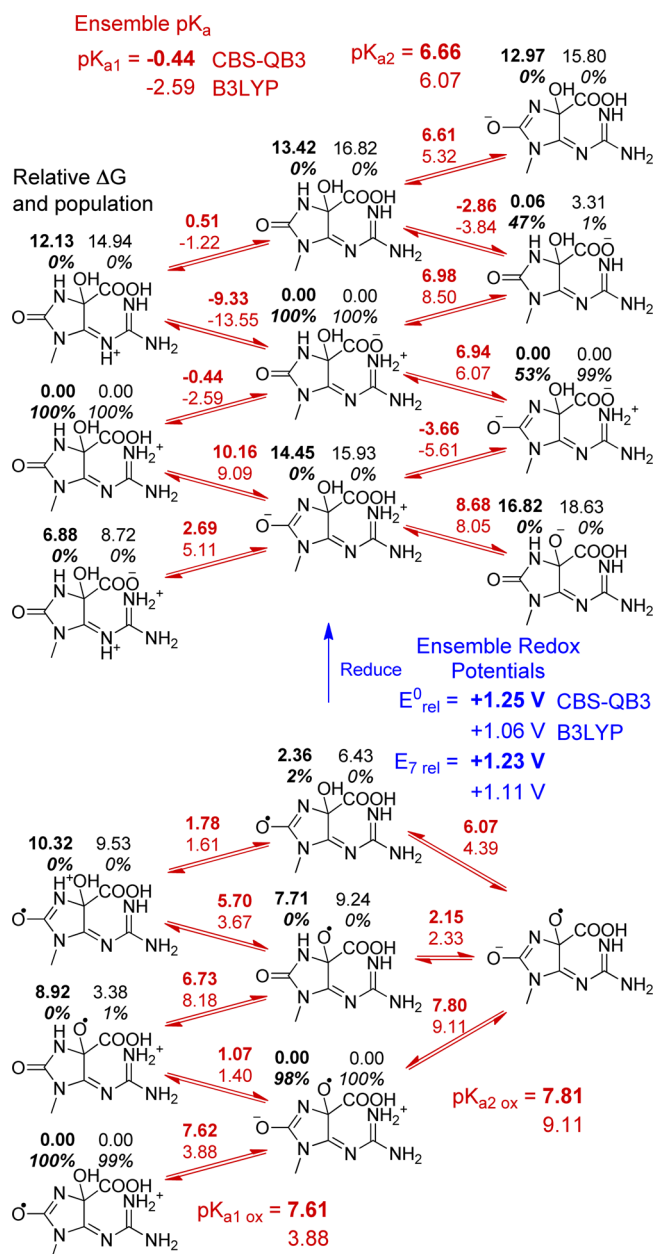
the 4-hydroxyl group has a p$K_{a1 ox}$ of 3.88−7.61, and deprotonation of the neutral radical at the guanidine group has a pK_{a2ox} of 7.81−9.11. This leads to a nominal E_7 value that is ca. 1.11−1.23 V higher than that of guanine. However, deprotonation of the carboxyl group in any of the 4carboxyGh radical species leads to decarboxylation. The E_7 for the oxidative process including decarboxylation to give oxidized neutral Gh is 0.01−0.10 V lower than E_7 for G.

Decarboxylation of 4carboxyGh and tautomerization produces guanidinohydantoin (Gh), and is exothermic by ca. 30 kcal/mol. For neutral Gh (Figure 8), the zwitterion is 3.6−5.1 kcal/mol more stable than the other tautomers. Deprotonation of the guanidine group has a pK_{a1} of 6.11−7.77, and deprotonation of the hydantoin group has a pK_{a2} of
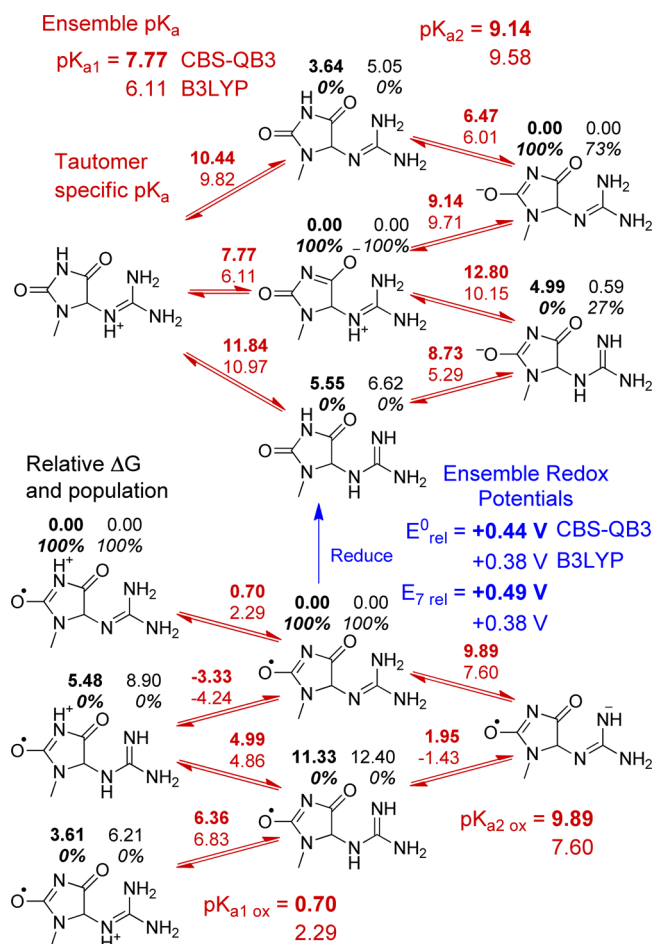
Figure 8. Calculated pK_a values and relative reduction potentials for 1-methylguanidinohydantoin (Gh). See Figure 2 caption for details.

Figure 9. Calculated pK_a values and relative reduction potentials for N-methylspiroiminodihydantoin (Sp). See Figure 2 caption for details.

9.14−9.58. There is no mention of any experimental measurements for the pK_a values of Gh in the literature. The pK_a values of guanidines can vary significantly with substituents (e.g., guanidine pK_a 13.7,[71] acetylguanidine pK_a 8.3 (experimental[72]) versus 8.5 (present calculations)) but the pK_a values of substituted hydantoins fall in a much narrower range (pK_a 8−10).[73−75] The calculated $pK_{a1\ ox}$ of 0.70−2.29 can be compared to $pK_{a1\ ox}$ values computed for guanine (2.53−3.34), 4carboxyGh (3.88−7.61), and 5OH8OG (2.31−5.23). Oxidized Gh is predicted to be neutral at pH 7, and E_7 is calculated to be 0.38−0.49 V higher than that of guanine.

As summarized in Figure 9, Sp is readily deprotonated, with pK_{a1} −0.06 to 1.32 and pK_{a2} 2.64−3.30. The values are in agreement with those calculated by Verdolino et al. (pK_{a1} 0.5 and pK_{a2} 4.8).[63] However, they pointed out that a pK_{a2} of 4.8 is "surprisingly low for a substituted hydantoin".[63] They attribute the low pK_{a2} value to through-space interactions of the C6 carbonyl group (confirmed by replacing C6−O6 with C=CH$_2$ and CH$_2$) and greater solvent stabilization of the N7 anion (tautomers with an N7 anion have a dipole moment of 15−20 debye compared to 5−15 debye for other tautomers).[63] The present calculations may underestimate pK_{a2}, and a better treatment of solvent effects may be needed. Verdolino et al. have estimated the pK_{a2} of Sp to be around 7. The calculated pK_a values of oxidized Sp are probably also too low because of similar effects described above for the pK_{a2}. Oxidized Sp is most likely an anion at pH 7, and E_7 is calculated to be 0.78−0.93 V higher than that of guanine.
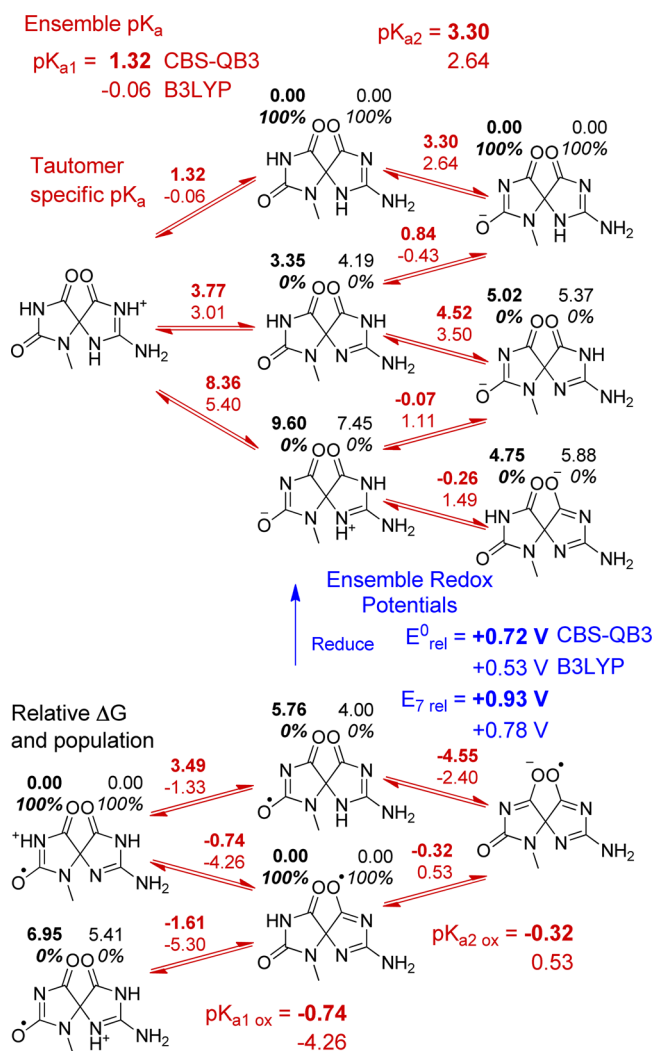
Pathway B. A key intermediate on the pathway to FAPyG is 2-amino-8-hydroxy-9-methyl-1,7,8-trihydropurin-6-one (hemiaminal), shown in Figure 10. The pK_a values of the hemiaminal (pK_{a1} 2.49−2.62, pK_{a2} 7.92−9.53) are similar to the pK_a values of guanine (pK_{a1} 3.20−3.50, pK_{a2} 9.10−9.34). All the ring nitrogens are protonated in the cation species, and the pK_{a1} corresponds to a deprotonation at N3. The next deprotonation for the pK_{a2} occurs at N1. The $pK_{a1\ ox}$ of the radical cation involves a deprotonation at the N7 position. Under very basic conditions, the neutral radical is predicted to deprotonate at the N1 position. The hemiaminal intermediate is very readily oxidized, and its E_7 value is 0.75−0.84 V lower than that of guanine. The hemiaminal intermediate is even more susceptible to oxidation than is 8oxoG. Tautomers with the C8-hydroxyl species deprotonated were difficult to obtain as many of the optimizations progressed toward ring-opening. Ring-opening at the C8−N9 bond of the hemiaminal and tautomerism leads to 2,6-diamino-(N-methyl)-5-formamido-4-hydroxypyrimidine (FAPyG) and is exothermic by ca. 9−11 kcal/mol. Breaking the N7−C8 bond followed by tautomerism yields 2,5-diamino-(N-methyl)-6-formamido-4-hydroxypyrimidine (2,5FAPyG) and is exothermic by ca. 4−6 kcal/mol.

The pK_a values for FAPyG (Figure 11) and 2,5FAPyG (Figure 12) are similar to one another in addition to being
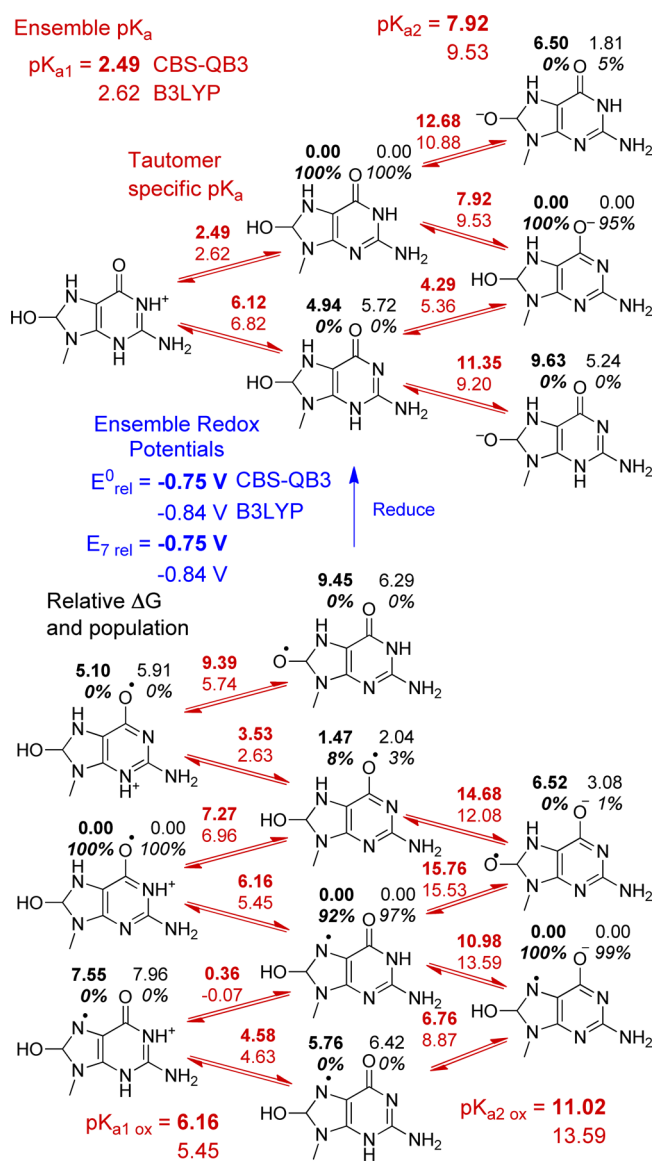
Figure 10. Calculated pK_a values and relative reduction potentials for 2-amino-8-hydroxy-9-methyl-1,7,8-trihydropurin-6-one (hemiaminal). See Figure 2 caption for details.

Figure 11. Calculated pK_a values and relative reduction potentials for 2,6-diamino-(N-methyl)-5-formamido-4-hydroxypyrimidine (FAPyG). See Figure 2 caption for details.

E_7 values of FAPyG and 2,5FAPyG are 0.25−0.32 V and 0.42−0.54 V lower than that of G, respectively. FAPyG has an E_7 that is 0.17−0.22 V higher than that of 2,5FAPyG, making its susceptibility to oxidation somewhat less than that of 2,5FAPyG.

Pathway C. Pathway C starts with oxidative damage caused by a reactive oxygen species attacking the C5 position of guanine to yield the 5-hydroxy-9-methylguanine (5OHG) intermediate shown in Figure 13. While the calculated pK_a values of 5OHG are similar to those of G and many of the other intermediates, the sites of protonation/deprotonation differ. 5OHG is protonated at N3 with a pK_{a1} of 2.77−3.69, whereas most of the other guanine oxidation intermediates are predominantly protonated at N1 or N7. The only acidic proton remaining in neutral 5OHG is the C5 hydroxyl which deprotonates at a pK_{a2} of 8.03−9.44. The oxidized radical cation prefers to be protonated at the N1 position and deprotonates with a pK_{a1} of 4.11−4.81. Additional tautomers of 5OHG radical cation (such as the isomer protonated at O5) could not be optimized because of ring-opening at the C5−C6 bond. Similarly, attempts at optimizing a 5OHG radical anion failed because of ring-opening for all structures considered. In the absence of ring-opening, the calculated E_7 value is 0.81−1.05 V higher than that of G.

Similar to the 5OH8OG-to-Sp conversion, 5OHG can undergo an acyl migration to yield N-methyl-2-deoxospiroiminodihydantoin

similar to the pK_a values of guanine. FAPyG and 2,5FAPyG are protonated under acidic conditions on the N1 position of the pyrimidine ring with calculated pK_{a1} values of 3.29−3.66 and 2.77−3.10, respectively. Neutral FAPyG and 2,5FAPyG deprotonate from the N3 position with calculated pK_{a2} values of 8.40−9.06 and 7.04−7.40, respectively. The calculated 2,5FAPyG pK_{a2} indicates a significant concentration of the anion should be present under physiological conditions. The radical cation species for FAPyG and 2,5FAPyG deprotonate at the N3 position with $pK_{a1\ ox}$ values of 5.41−6.58 and 4.11−4.43, respectively, which are slightly more basic than the radical cations of other guanine species (ca. 3−4). The oxidized neutral FAPyG deprotonates from the formamide group at a $pK_{a2\ ox}$ of 8.08. The deprotonation of oxidized neutral 2,5FAPyG takes place at the same site (formerly the N7 nitrogen atom) with a very similar $pK_{a2\ ox}$ of 8.58−8.61 despite the fact that the site is an amino group rather than an amide. In agreement with the computational study by Munk et al.,[20] FAPyG is the thermodynamically favored product by ca. 5.4−8.5 kcal/mol.
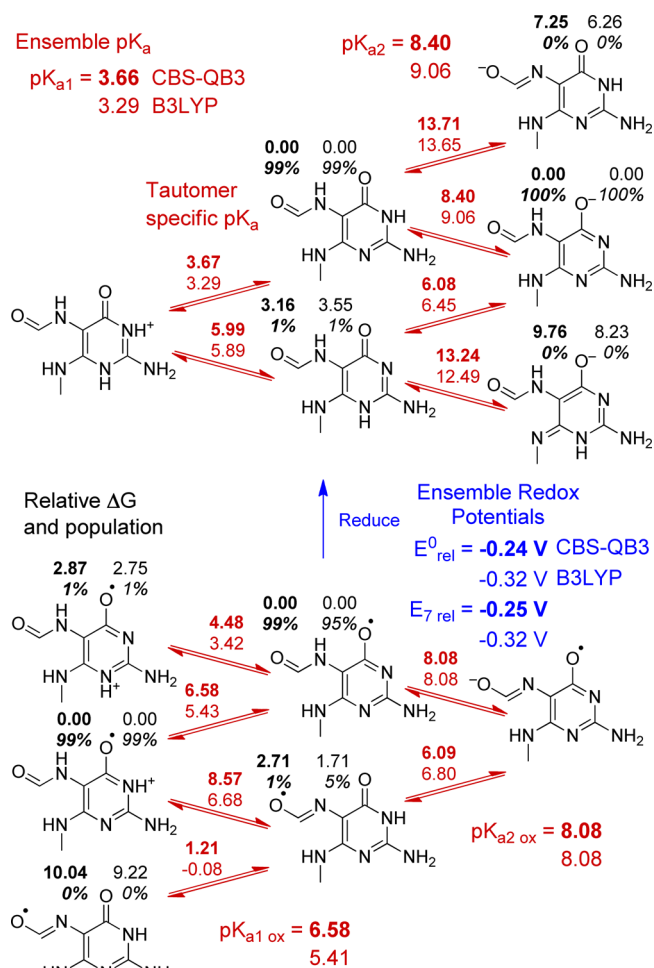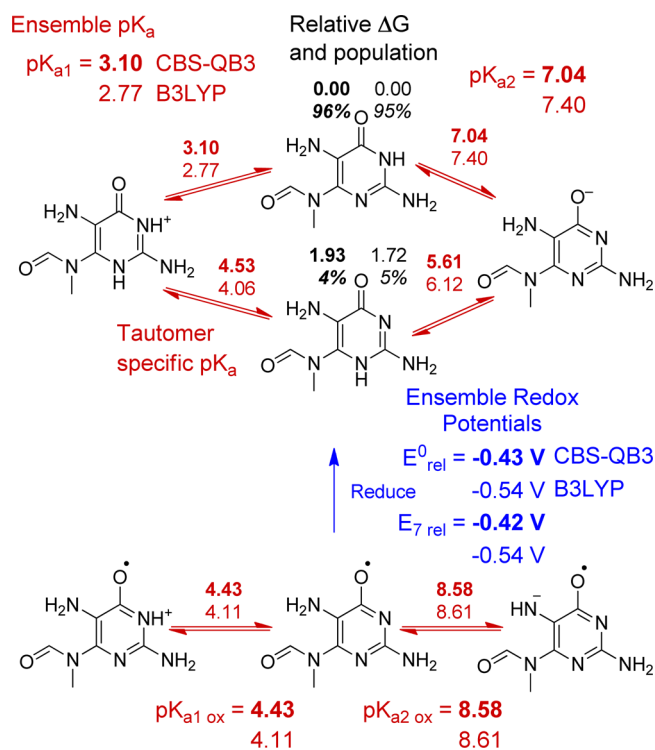
Figure 12. Calculated pK_a values and relative reduction potentials for 2,5-diamino-(N-methyl)-6-formamido-4-hydroxypyrimidine (2,5FAPyG). See Figure 2 caption for details.
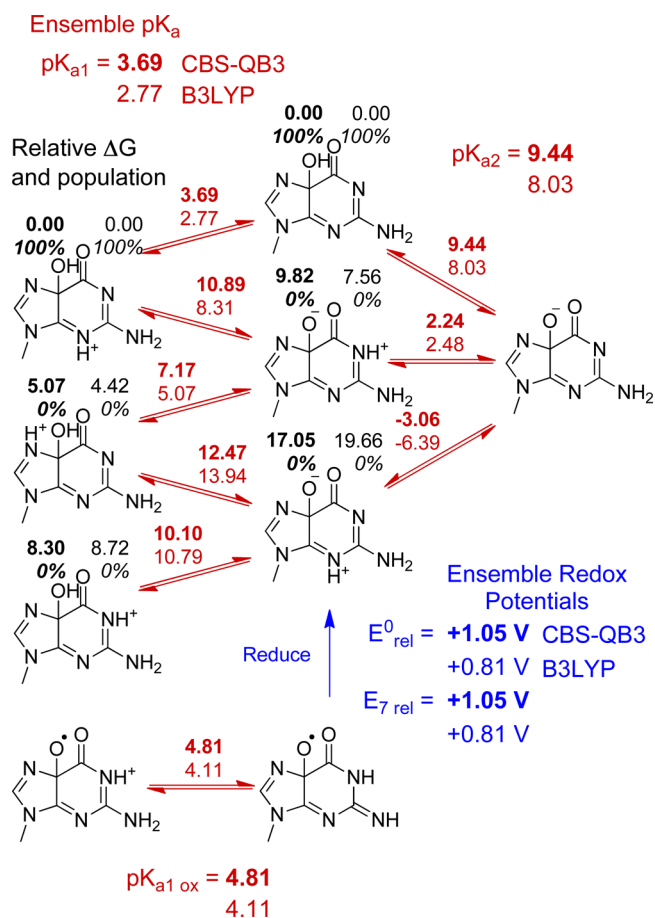

Figure 13. Calculated pK_a values and relative reduction potentials for 5-hydroxy-9-methylguanine (5OHG). See Figure 2 caption for details.
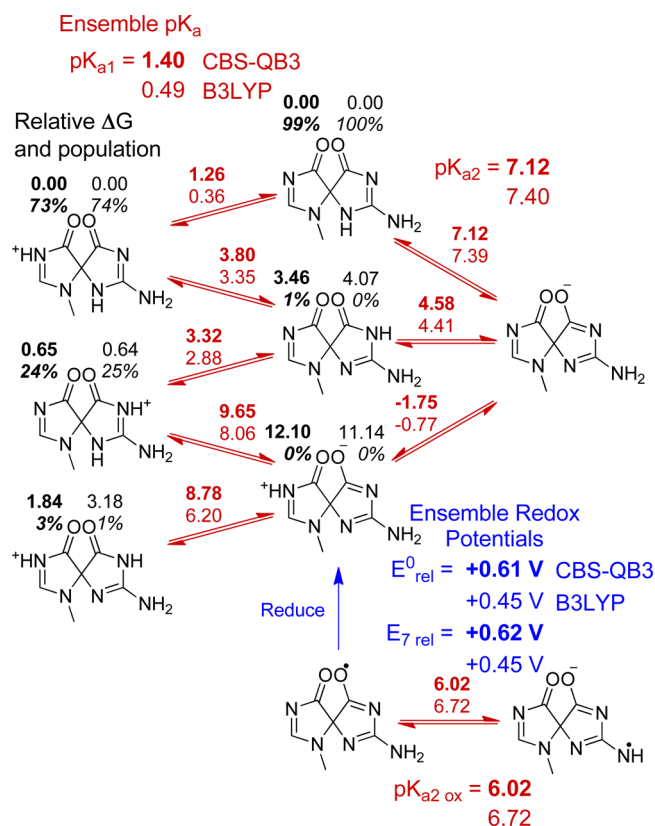

Figure 14. Calculated pK_a values and relative reduction potentials for N-methyl-2-deoxo-spiroiminodihydantoin (Sp$_{red}$). See Figure 2 caption for details.
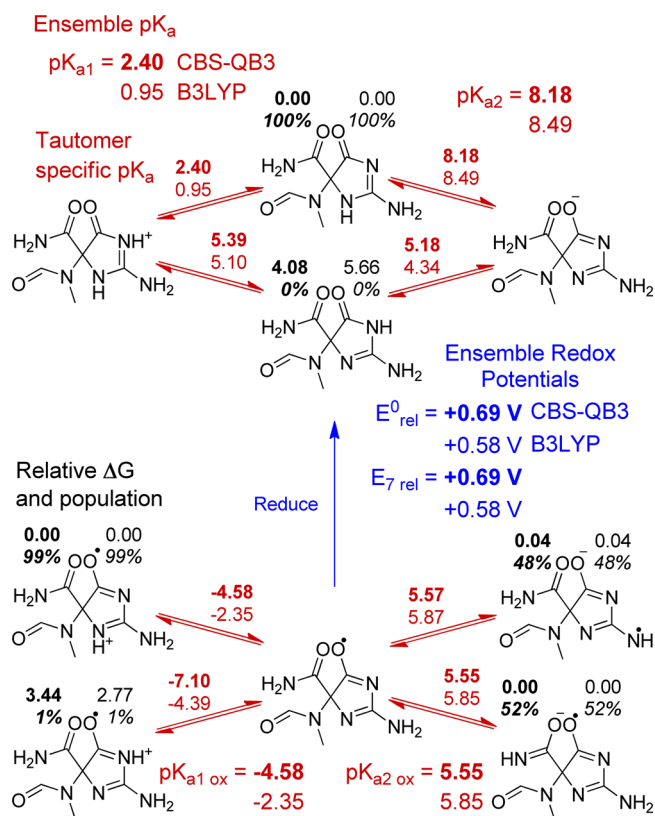

Figure 15. Calculated pK_a values and relative reduction potentials for 5-carboxamido-5-formamido-(N-methyl)-2-iminohydantoin (2Ih). See Figure 2 caption for details.
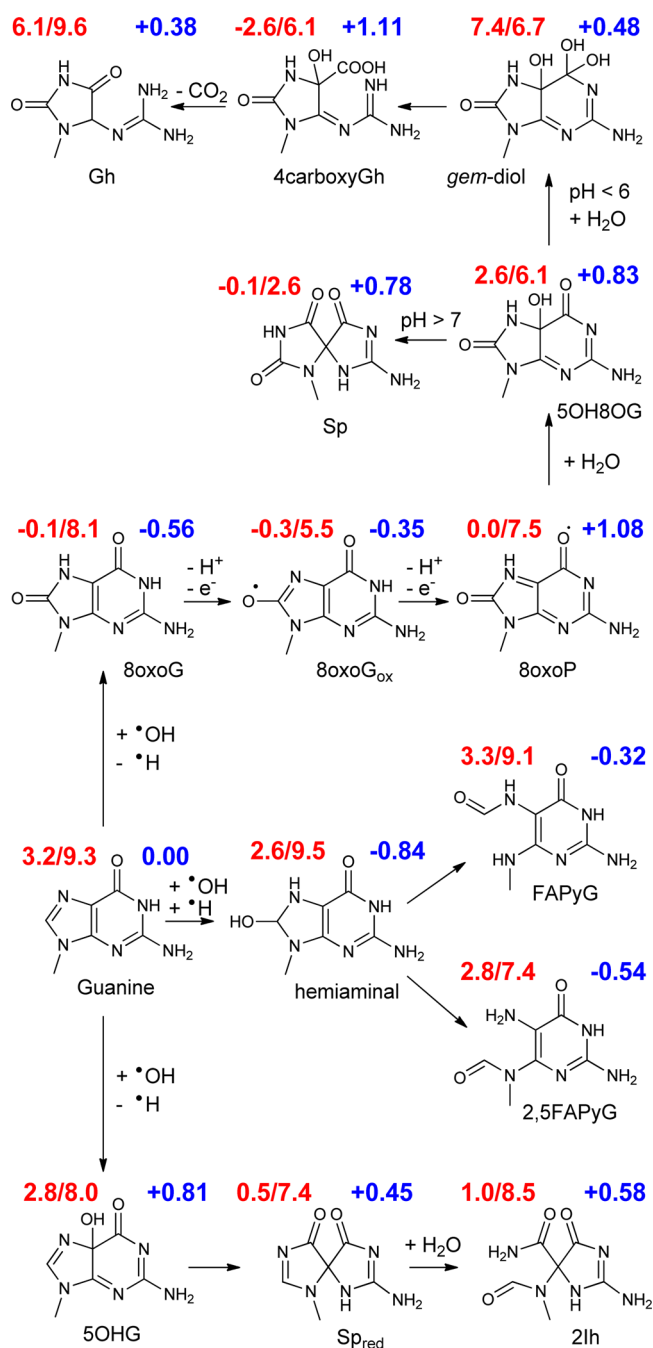
Figure 16. Summary of the pK_a (red) and E_7 values relative to guanine (blue) for key intermediates and products along three pathways for guanine oxidation.

(i.e., reduced spiroiminodihydantoin or Sp_{red}). This reaction is exothermic by 20−21 kcal/mol. Sp_{red} has three ring nitrogens that are reasonable protonation sites under physiological conditions. Two of three combinations of two protons on the three ring nitrogen sites are calculated to be similar in energy (Figure 14). Sp_{red} protonates at the guanidine group with a pK_{a1} of 0.49−1.40. Neutral Sp_{red} deprotonates at the former N3 with a pK_{a2} of 7.12−7.40. An oxidized radical cation isomer of Sp_{red} could not be optimized because of the instabilities in the rings leading to ring-opening. Oxidation coupled with loss of a proton leads to the neutral radical of Sp_{red}, which can be optimized. The calculated $pK_{a2\ ox}$ for the neutral radical is 6.02−6.72, indicating that it would lose another proton at physiological conditions, yielding the radical

anion species. The calculated E_7 for Sp_{red} is 0.45−0.62 V higher than the calculated potential for G.

The final product in pathway C involves a water addition across the C2−N3 bond of the deaminated hydantoin ring followed by proton transfer and ring-opening to the 5-carboxamido-5-formamido-(N-methyl)-2-iminohydantoin (2Ih) product. This reaction is calculated to be endothermic by 3−6 kcal/mol. Similar to Sp and Sp_{red}, the predicted pK_{a1} of 2Ih is acidic with a calculated value of 0.95−2.40, and 2Ih is predicted to deprotonate from the former N1 position (Figure 15). 2Ih deprotonates from the former N3 position with a calculated pK_{a2} of 8.18−8.49. The oxidized radical cation also has a predicted acidic $pK_{a1\ ox}$ of −4.58 to −2.35 for deprotonation at the former N3 position. The neutral 2Ih radical species can deprotonate from either of the exocyclic amino groups with almost equal energy. The calculated $pK_{a2\ ox}$ is 5.55−5.85 and is similar to the calculated $pK_{a2\ ox}$ of Sp_{red}. The calculated E_7 value of 2Ih is also very similar to that of the Sp_{red} species and is 0.58−0.69 V higher than that of guanine, indicating that further oxidation of 2Ih is unlikely.

■ CONCLUSIONS

Three major reaction pathways resulting from the initial oxidation of guanine were investigated, and the reduction potentials and pK_a values of transient intermediates and products were calculated using the scheme developed in our earlier paper. The approach uses high-level ab initio and DFT electronic structure calculations and an implicit solvation model with cavity scaling. The study incorporates computed tautomerization energies to calculate $E°$ and pK_a values and to obtain E_7 values that can be compared with experimental measurements in aqueous solution. The B3LYP results are summarized in Figure 16. Pathway A starts at 8-oxoguanine (8oxoG). The calculations show that 8oxoG can easily lose an electron followed by the loss of two protons and the loss of another electron to produce 8-oxopurine (8oxoP). The calculated reduction potentials for subsequent intermediates along pathway A are 0.4−1.1 V higher than that of guanine, indicating that they will most likely not be oxidized further. Pathway A branches at 5-hydroxy-8-oxoguanine (5OH8OG), leading to guanidinohydantoin (Gh) at low pH and spiroiminodihydantoin (Sp) at high pH. The calculated pK_a of 6.1 for 5OH8OG is in good agreement with a pK_a of 5.7 inferred from the experimental dependence of the branching ratio on the pH. Pathway B leads to two formamidopyrimidine isomers (FAPyG and 2,5FAPyG) through a hemiaminal intermediate. These species have reduction potentials 0.3−0.8 V lower than that of guanine. This is in accord with experimental observations that FAPyG products are favored by anaerobic environments. Pathway C starts with 5-hydroxy-guanine, goes through the reduced spiroiminodihydantoin intermediate (Sp_{red}), and ends at the 5-carboxamido-5-formamido-2-iminohydantoin product (2Ih). The computed E_7 values are 0.4−0.8 V higher than that of guanine, indicating that further oxidation of the intermediates is unlikely.

■ ASSOCIATED CONTENT

S Supporting Information

A spreadsheet containing the energetic data and calculations of the pK_a values and reduction potentials. This material is available free of charge via the Internet at http://pubs.acs.org.

■ AUTHOR INFORMATION

Notes
The authors declare no competing financial interest.

■ REFERENCES

(1) Ames, B. N.; Shigenaga, M. K.; Hagen, T. M. Oxidants, Antioxidants, and the Degenerative Diseases of Aging. *Proc. Natl. Acad. Sci., U.S.A.* **1993**, *90*, 7915−7922.

(2) Breen, A. P.; Murphy, J. A. Reactions of Oxyl Radicals with DNA. *Free Radical Biol. Med.* **1995**, *18*, 1033−1077.

(3) Cadet, J.; Berger, M.; Douki, T.; Morin, B.; Raoul, S.; Ravanat, J. L.; Spinelli, S. Effects of UV and Visible Radiation on DNA: Final Base Damage. *Biol. Chem.* **1997**, *378*, 1275−1286.

(4) Burrows, C. J.; Muller, J. G. Oxidative Nucleobase Modifications Leading to Strand Scission. *Chem. Rev.* **1998**, *98*, 1109−1151.

(5) Cooke, M. S.; Olinski, R.; Evans, M. D. Does Measurement of Oxidative Damage to DNA Have Clinical Significance? *Clin. Chim. Acta* **2006**, *365*, 30−49.

(6) Gimisis, T.; Cismas, C. Isolation, Characterization, and Independent Synthesis of Guanine Oxidation Products. *Eur. J. Org. Chem.* **2006**, 1351−1378.

(7) Pratviel, G.; Meunier, B. Guanine Oxidation: One- and Two-Electron Reactions. *Chem.—Eur. J.* **2006**, *12*, 6018−6030.

(8) Son, J.; Pang, B.; McFaline, J. L.; Taghizadeh, K.; Dedon, P. C. Surveying the Damage: The Challenges of Developing Nucleic Acid Biomarkers of Inflammation. *Mol. Biosyst.* **2008**, *4*, 902−908.

(9) Lonkar, P.; Dedon, P. C. Reactive Species and DNA Damage in Chronic Inflammation: Reconciling Chemical Mechanisms and Biological Fates. *Int. J. Cancer* **2011**, *128*, 1999−2009.

(10) Steenken, S. Purine Bases, Nucleosides, and Nucleotides: Aqueous Solution Redox Chemistry and Transformation Reactions of Their Radical Cations and e⁻ and OH Adducts. *Chem. Rev.* **1989**, *89*, 503−520.

(11) Candeias, L. P.; Steenken, S. Reaction of HO● with Guanine Derivatives in Aqueous Solution: Formation of Two Different Redox-Active OH-Adduct Radicals and Their Unimolecular Transformation Reactions. Properties of G(-H)●. *Chem.—Eur. J.* **2000**, *6*, 475−484.

(12) Luo, W. C.; Muller, J. G.; Rachlin, E. M.; Burrows, C. J. Characterization of Spiroiminodihydantoin as a Product of One-Electron Oxidation of 8-Oxo-7,8-dihydroguanosine. *Org. Lett.* **2000**, *2*, 613−616.

(13) Llano, J.; Eriksson, L. A. Oxidation Pathways of Adenine and Guanine in Aqueous Solution from First Principles Electrochemistry. *Phys. Chem. Chem. Phys.* **2004**, *6*, 4707−4713.

(14) Crean, C.; Geacintov, N. E.; Shafirovich, V. Oxidation of Guanine and 8-Oxo-7,8-dihydroguanine by Carbonate Radical Anions: Insight from Oxygen-18 Labeling Experiments. *Angew. Chem., Int. Ed.* **2005**, *44*, 5057−5060.

(15) Fleming, A. M.; Muller, J. G.; Ji, I. S.; Burrows, C. J. Characterization of 2′-Deoxyguanosine Oxidation Products Observed in the Fenton-like System Cu(II)/H₂O₂/Reductant in Nucleoside and Oligodeoxynucleotide Contexts. *Org. Biomol. Chem.* **2011**, *9*, 3338−3348.

(16) Delaney, S.; Jarem, D. A.; Volle, C. B.; Yennie, C. J. Chemical and Biological Consequences of Oxidatively Damaged Guanine in DNA. *Free Radical Res.* **2012**, *46*, 420−441.

(17) Jena, N. R.; Mishra, P. C. Formation of Ring-Opened and Rearranged Products of Guanine: Mechanisms and Biological Significance. *Free Radical Biol. Med.* **2012**, *53*, 81−94.

(18) Wetmore, S. D.; Boyd, R. J.; Eriksson, L. A. Comparison of Experimental and Calculated Hyperfine Coupling Constants. Which Radicals Are Formed in Irradiated Guanine? *J. Phys. Chem. B* **1998**, *102*, 9332−9343.

(19) Wetmore, S. D.; Boyd, R. J.; Llano, J.; Lundqvist, M. J.; Eriksson, L. A. Hydroxyl Radical Reactions in Biological Media. In *Recent Advances in Density Functional Methods*; Barone, V., Bencini, A., Fantucci, P., Eds.; World Scientific: Singapore, 2000; Vol. 3, pp 387−415.

(20) Munk, B. H.; Burrows, C. J.; Schlegel, H. B. Exploration of Mechanisms for the Transformation of 8-Hydroxy Guanine Radical to FAPyG by Density Functional Theory. *Chem. Res. Toxicol.* **2007**, *20*, 432−444.

(21) Munk, B. H.; Burrows, C. J.; Schlegel, H. B. An Exploration of Mechanisms for the Transformation of 8-Oxoguanine to Guanidino-hydantoin and Spiroiminodihydantoin by Density Functional Theory. *J. Am. Chem. Soc.* **2008**, *130*, 5245−5256.

(22) Ye, Y.; Munk, B. H.; Muller, J. G.; Cogbill, A.; Burrows, C. J.; Schlegel, H. B. Mechanistic Aspects of the Formation of Guanidinohydantoin from Spiroiminodihydantoin under Acidic Conditions. *Chem. Res. Toxicol.* **2009**, *22*, 526−535.

(23) Jovanovic, S. V.; Simic, M. G. One-Electron Redox Potentials of Purines and Pyrimidines. *J. Phys. Chem.* **1986**, *90*, 974−978.

(24) Faraggi, M.; Broitman, F.; Trent, J. B.; Klapper, M. H. One-Electron Oxidation Reactions of Some Purine and Pyrimidine Bases in Aqueous Solutions. Electrochemical and Pulse Radiolysis Studies. *J. Phys. Chem.* **1996**, *100*, 14751−14761.

(25) Seidel, C. A. M.; Schulz, A.; Sauer, M. H. M. Nucleobase-Specific Quenching of Fluorescent Dyes. 1. Nucleobase One-Electron Redox Potentials and Their Correlation with Static and Dynamic Quenching Efficiencies. *J. Phys. Chem.* **1996**, *100*, 5541−5553.

(26) Steenken, S.; Jovanovic, S. V. How Easily Oxidizable Is DNA? One-Electron Reduction Potentials of Adenosine and Guanosine Radicals in Aqueous Solution. *J. Am. Chem. Soc.* **1997**, *119*, 617−618.

(27) Steenken, S.; Jovanovic, S. V.; Bietti, M.; Bernhard, K. The Trap Depth (in DNA) of 8-Oxo-7,8-dihydro-2′-deoxyguanosine as Derived from Electron-Transfer Equilibria in Aqueous Solution. *J. Am. Chem. Soc.* **2000**, *122*, 2373−2374.

(28) Oliveira-Brett, A. M.; Piedade, J. A. P.; Silva, L. A.; Diculescu, V. C. Voltammetric Determination of All DNA Nucleotides. *Anal. Biochem.* **2004**, *332*, 321−329.

(29) Fukuzumi, S.; Miyao, H.; Ohkubo, K.; Suenobu, T. Electron-Transfer Oxidation Properties of DNA Bases and DNA Oligomers. *J. Phys. Chem. A* **2005**, *109*, 3285−3294.

(30) Langmaier, J.; Samec, Z.; Samcova, E.; Hobza, P.; Reha, D. Origin of Difference between One-Electron Redox Potentials of Guanosine and Guanine: Electrochemical and Quantum Chemical Study. *J. Phys. Chem. B* **2004**, *108*, 15896−15899.

(31) Gryn'ova, G.; Marshall, D. L.; Blanksby, S. J.; Coote, M. L. Switching Radical Stability by pH-Induced Orbital Conversion. *Nat. Chem.* **2013**, *5*, 474−481.

(32) Caruso, T.; Carotenuto, M.; Vasca, E.; Peluso, A. Direct Experimental Observation of the Effect of the Base Pairing on the Oxidation Potential of Guanine. *J. Am. Chem. Soc.* **2005**, *127*, 15040−15041.

(33) Crespo-Hernandez, C. E.; Close, D. M.; Gorb, L.; Leszczynski, J. Determination of Redox Potentials for the Watson−Crick Base Pairs, DNA Nucleosides, and Relevant Nucleoside Analogues. *J. Phys. Chem. B* **2007**, *111*, 5386−5395.

(34) Psciuk, B. T.; Lord, R. L.; Munk, B. H.; Schlegel, H. B. Theoretical Determination of One-Electron Oxidation Potentials for Nucleic Acid Bases. *J. Chem. Theory Comput.* **2012**, *8*, 5107−5123.

(35) Bennaim, A.; Marcus, Y. Solvation Thermodynamics of Nonionic Solutes. *J. Chem. Phys.* **1984**, *81*, 2016−2027.

(36) Lewis, A.; Bumpus, J. A.; Truhlar, D. G.; Cramer, C. J. Molecular Modeling of Environmentally Important Processes: Reduction Potentials. *J. Chem. Educ.* **2004**, *81*, 596−604.

(37) Lewis, A.; Bumpus, J. A.; Truhlar, D. G.; Cramer, C. J. *J. Chem. Educ.* 2004, 81, 596−604. *J. Chem. Educ.* **2007**, *84*, 934−934.

(38) Kelly, C. P.; Cramer, C. J.; Truhlar, D. G. Aqueous Solvation Free Energies of Ions and Ion−Water Clusters Based on an Accurate Value for the Absolute Aqueous Solvation Free Energy of the Proton. *J. Phys. Chem. B* **2006**, *110*, 16066−16081.

9530

dx.doi.org/10.1021/jp4062412 | *J. Phys. Chem. B* 2013, 117, 9518−9531

(39) Isse, A. A.; Gennaro, A. Absolute Potential of the Standard Hydrogen Electrode and the Problem of Interconversion of Potentials in Different Solvents. *J. Phys. Chem. B* **2010**, *114*, 7894−7899.

(40) Vosko, S. H.; Wilk, L.; Nusair, M. Accurate Spin-Dependent Electron Liquid Correlation Energies for Local Spin-Density Calculations: A Critical Analysis. *Can. J. Phys.* **1980**, *58*, 1200−1211.

(41) Becke, A. D. Density-Functional Exchange-Energy Approximation with Correct Asymptotic Behavior. *Phys. Rev. A* **1988**, *38*, 3098−3100.

(42) Lee, C. T.; Yang, W. T.; Parr, R. G. Development of the Colle−Salvetti Correlation-Energy Formula into a Functional of the Electron-Density. *Phys. Rev. B* **1988**, *37*, 785−789.

(43) Becke, A. D. Density-Functional Thermochemistry. 3. The Role of Exact Exchange. *J. Chem. Phys.* **1993**, *98*, 5648−5652.

(44) Stephens, P. J.; Devlin, F. J.; Chabalowski, C. F.; Frisch, M. J. *Ab Initio* Calculations of Vibrational Absorption and Circular-Dichroism Spectra Using Density Functional Force Fields. *J. Phys. Chem.* **1994**, *98*, 11623−11627.

(45) Ditchfield, R.; Hehre, W. J.; Pople, J. A. Self-Consistent Molecular-Orbital Methods. IX. An Extended Gaussian-Type Basis for Molecular-Orbital Studies of Organic Molecules. *J. Chem. Phys.* **1971**, *54*, 724−728.

(46) Hehre, W. J.; Ditchfield, R.; Pople, J. A. Self-Consistent Molecular-Orbital Methods. XII. Further Extensions of Gaussian-Type Basis Sets for Use in Molecular Orbital Studies of Organic Molecules. *J. Chem. Phys.* **1972**, *56*, 2257.

(47) Hariharan, P. C.; Pople, J. A. Influence of Polarization Functions on Molecular-Orbital Hydrogenation Energies. *Theor. Chim. Acta* **1973**, *28*, 213−222.

(48) Hariharan, P. C.; Pople, J. A. Accuracy of AH Equilibrium Geometries by Single Determinant Molecular-Orbital Theory. *Mol. Phys.* **1974**, *27*, 209−214.

(49) Gordon, M. S. The Isomers of Silacyclopropane. *Chem. Phys. Lett.* **1980**, *76*, 163−168.

(50) Francl, M. M.; Pietro, W. J.; Hehre, W. J.; Binkley, J. S.; Gordon, M. S.; Defrees, D. J.; Pople, J. A. Self-Consistent Molecular-Orbital Methods. XXIII. A Polarization-Type Basis Set for Second-Row Elements. *J. Chem. Phys.* **1982**, *77*, 3654−3665.

(51) Kendall, R. A.; Dunning, T. H.; Harrison, R. J. Electron-Affinities of the First-Row Atoms Revisited. Systematic Basis-Sets and Wave-Functions. *J. Chem. Phys.* **1992**, *96*, 6796−6806.

(52) Montgomery, J. A.; Frisch, M. J.; Ochterski, J. W.; Petersson, G. A. A Complete Basis Set Model Chemistry. VI. Use of Density Functional Geometries and Frequencies. *J. Chem. Phys.* **1999**, *110*, 2822−2827.

(53) Montgomery, J. A.; Frisch, M. J.; Ochterski, J. W.; Petersson, G. A. A Complete Basis Set Model Chemistry. VII. Use of the Minimum Population Localization Method. *J. Chem. Phys.* **2000**, *112*, 6532−6542.

(54) Marenich, A. V.; Cramer, C. J.; Truhlar, D. G. Universal Solvation Model Based on Solute Electron Density and on a Continuum Model of the Solvent Defined by the Bulk Dielectric Constant and Atomic Surface Tensions. *J. Phys. Chem. B* **2009**, *113*, 6378−6396.

(55) Cances, E.; Mennucci, B.; Tomasi, J. A New Integral Equation Formalism for the Polarizable Continuum Model: Theoretical Background and Applications to Isotropic and Anisotropic Dielectrics. *J. Chem. Phys.* **1997**, *107*, 3032−3041.

(56) Mennucci, B.; Tomasi, J. Continuum Solvation Models: A New Approach to the Problem of Solute's Charge Distribution and Cavity Boundaries. *J. Chem. Phys.* **1997**, *106*, 5151−5158.

(57) Cossi, M.; Barone, V.; Mennucci, B.; Tomasi, J. Ab Initio Study of Ionic Solutions by a Polarizable Continuum Dielectric Model. *Chem. Phys. Lett.* **1998**, *286*, 253−260.

(58) Scalmani, G.; Frisch, M. J. Continuous Surface Charge Polarizable Continuum Models of Solvation. I. General Formalism. *J. Chem. Phys.* **2010**, *132*, 114110.

(59) Frisch, M. J.; Trucks, G. W.; Schlegel, H. B.; Scuseria, G. E.; Robb, M. A.; et al. *Gaussian Development Version*, revision H.20+; Gaussian, Inc.: Wallingford, CT, 2010.

(60) Clark, W. M. *Oxidation-Reduction Potentials of Organic Systems*; Williams & Wilkins: Baltimore, MD, 1960.

(61) Wardman, P. Reduction Potentials of One-Electron Couples Involving Free-Radicals in Aqueous-Solution. *J. Phys. Chem. Ref. Data* **1989**, *18*, 1637−1755.

(62) Camaioni, D. M.; Schwerdtfeger, C. A. Comment on "Accurate Experimental Values for the Free Energies of Hydration of H⁺, OH⁻, and H₃O⁺". *J. Phys. Chem. A* **2005**, *109*, 10795−10797.

(63) Verdolino, V.; Cammi, R.; Munk, B. H.; Schlegel, H. B. Calculation of pKₐ Values of Nucleobases and the Guanine Oxidation Products Guanidinohydantoin and Spiroiminodihydantoin Using Density Functional Theory and a Polarizable Continuum Model. *J. Phys. Chem. B* **2008**, *112*, 16860−16873.

(64) Jang, Y. H.; Goddard, W. A.; Noyes, K. T.; Sowers, L. C.; Hwang, S.; Chung, D. S. pKₐ Values of Guanine in Water: Density Functional Theory Calculations Combined with Poisson−Boltzmann Continuum−Solvation Model. *J. Phys. Chem. B* **2003**, *107*, 344−357.

(65) Song, B.; Zhao, J.; Griesser, R.; Meiser, C.; Sigel, H.; Lippert, B. Effects of (N7)-Coordinated Nickel(II), Copper(II), or Platinum(II) on the Acid-Base Properties of Guanine Derivatives and Other Related Purines. *Chem.—Eur. J.* **1999**, *5*, 2374−2387.

(66) Baik, M. H.; Silverman, J. S.; Yang, I. V.; Ropp, P. A.; Szalai, V. A.; Yang, W. T.; Thorp, H. H. Using Density Functional Theory to Design DNA Base Analogues with Low Oxidation Potentials. *J. Phys. Chem. B* **2001**, *105*, 6437−6444.

(67) Christensen, J. J.; Rytting, J. H.; Izatt, R. M. Thermodynamic pK, ΔH°, ΔS°, and ΔCₚ° Values for Proton Dissociation from Several Purines and Their Nucleosides in Aqueous Solution. *Biochemistry* **1970**, *9*, 4907−4913.

(68) Cho, B. P. Structure of Oxidatively Damaged Nucleic-Acid Adducts: pH-Dependence of the C-13 NMR-Spectra of 8-Oxoguanosine and 8-Oxoadenosine. *Magn. Reson. Chem.* **1993**, *31*, 1048−1053.

(69) Jang, Y. H.; Goddard, W. A.; Noyes, K. T.; Sowers, L. C.; Hwang, S.; Chung, D. S. First Principles Calculations of the Tautomers and pKₐ Values of 8-Oxoguanine: Implications for Mutagenicity and Repair. *Chem. Res. Toxicol.* **2002**, *15*, 1023−1035.

(70) Fleming, A. M.; Muller, J. G.; Dlouhy, A. C.; Burrows, C. J. Structural Context Effects in the Oxidation of 8-Oxo-7,8-dihydro-2′-deoxyguanosine to Hydantoin Products: Electrostatics, Base Stacking, and Base Pairing. *J. Am. Chem. Soc.* **2012**, *134*, 15091−15102.

(71) Shugar, D.; Fox, J. J. Spectrophotometric Studies of Nucleic Acid Derivatives and Related Compounds as a Function of pH. I. Pyrimidines. *Biochim. Biophys. Acta* **1952**, *9*, 199−218.

(72) Albert, A.; Goldacre, R.; Phillips, J. The Strength of Heterocyclic Bases. *J. Chem. Soc.* **1948**, 2240−2249.

(73) Edward, J. T.; Nielsen, S.; Thiohydantoins, I. Ionization and ultraviolet absorption. *J. Chem. Soc.* **1957**, 5075−5079.

(74) Budavari, S. *The Merck Index*, 12th ed.; Merck: Whitehouse Station, NJ, 1996.

(75) Nosheen, E.; Shah, A.; Badshah, A.; Zia ur, R.; Hussain, H.; Qureshi, R.; Ali, S.; Siddiq, M.; Khan, A. M. Electrochemical Oxidation of Hydantoins at Glassy Carbon Electrode. *Electrochim. Acta* **2012**, *80*, 108−117.